ARTICLE

Solvent Dependence of Photophysical and Photochemical Behaviors of Thioxanthen-9-one

Lin Chen[a*], Lei Wang[b], Min Zheng[b], Lin Wang[a]

a. School of Physics and Materials Engineering, Hefei Normal University, Hefei 230601, China
b. Hefei National Laboratory for Physical Sciences at the Microscale and Department of Chemical Physics, University of Science and Technology of China, Hefei 230026, China

(Dated: Received on April 28, 2020; Accepted on June 14, 2020)

The photophysical and photochemical behaviors of thioxanthen-9-one (TX) in different solvents have been studied using nanosecond transient absorption spectroscopy. A unique absorption of the triplet state ^{3}TX* is observed, which involves two components, ^{3}nπ^* and $^3\pi\pi^*$ states. The $^3\pi\pi^*$ component contributes more to the ^{3}TX* when increasing the solvent polarity. The self-quenching rate constant k_{sq} of ^{3}TX* is decreased in the order of CH_3CN, CH_3CN/CH_3OH (1:1), and CH_3CN/H_2O (1:1), which might be caused by the exciplex formed from hydrogen bond interaction. In the presence of diphenylamine (DPA), the quenching of ^{3}TX* happens efficiently via electron transfer, producing the $TX^{\cdot-}$ anion and $DPA^{\cdot+}$ cation radicals. Because of insignificant solvent effects on the electron transfer, the electron affinity of the ^{3}nπ^* state is proved to be approximately equal to that of the $^3\pi\pi^*$ state. However, a solvent dependence is found in the dynamic decay of $TX^{\cdot-}$ anion radical. In the strongly acid aqueous acetonitrile (pH=3.0), a dynamic equilibrium between protonated and unprotonated TX is definitely observed. Once photolysis, $^3TXH^{+*}$ is produced, which contributes to the new band at 520 nm.

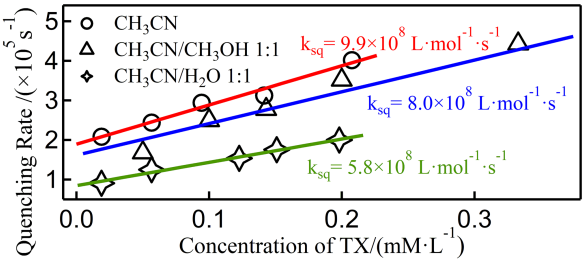

Key words: Solvent dependence, Electron transfer, Protonation, Hydrogen bonding, Transient absorption spectrum

I. INTRODUCTION

Solvent dependence plays a significant role in photophysics and photochemistry. Basically, the solvent polarity can influence the energies of the ground and excited states of molecules more or less [1−4]. For example, thioxanthone (thioxanthen-9-one, TX, Scheme 1) has drawn many theoretical and experimental studies [5−9]. Its first absorption band involves two transition components, nπ^* and $\pi\pi^*$ states [8−10]. Usually, the nπ^* state is the lowest in non-polar solvents, and the energy difference between nπ^* and $\pi\pi^*$ is rather small [9]. However, with the increase of solvent polarity, the $\pi\pi^*$ state is stabilized more efficiently rather than the nπ^* state [10]. As a result, $\pi\pi^*$ becomes the most stabilized state in polar solvents, and the energy gap is much larger [10]. Notably, a visible solvent effect has also been reported in deactivation of the singlet excited state TX (^{1}TX*). In polar solvents, the fluorescence is dominant, rather than the intersystem crossing (ISC) to ^{3}TX* [8, 9]. Thus, the strong fluorescence emission can be observed in polar solvents, whereas it becomes extremely weak in nonpolar solvents [9]. Moreover, the ^{3}TX* self-quenching rate constant (k_{sq}) has been mea-

*Author to whom correspondence should be addressed. E-mail: chenlin@hfnu.edu.cn

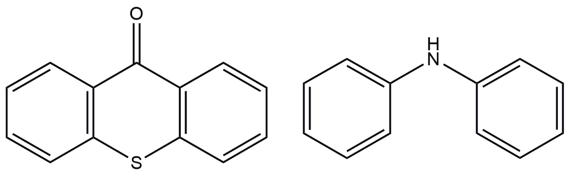

Scheme 1. Structures of thioxanthone (TX, left) and diphenylamine (DPA, right).

sured in different solvents, however, the mechanism of the $^3TX^*$ self-quenching process cannot be elucidated [11].

TX has often been used as photoinitiator in the photopolymerization systems [12−15]. The polymerization readily occurs in the presence of the coinitiator that behaves as an electron donor. Aliphatic amines are generally employed as coinitiators [16−19]. TX acquires industrial importance as radical sources, in combination with amines under UV irradiation [12]. The rate of the photopolymerization depends on the electron donor capacity of the amine, the electroaffinity of the photoinitiator, and the characteristics of the solvent [20−22]. To a large extent, the photophysical properties of TX depend on the polarity of the environment [8−10]. Thus it is worth investigating the solvent dependence on the reaction between TX and amine, leading to the efficiency optimization of the photoinitiators.

Diphenylamine (DPA, Scheme 1), as a representative amine, has often been chosen to play an electron donor role due to its low ionization potential. The previous studies [23−28] have confirmed that the ketonic oxygen of TX can easily capture an electron from amines like DPA. Using transient absorption spectroscopy, three absorption peaks of the $TX^{\cdot-}$ anion radical (680 nm), $DPA^{\cdot+}$ cation radical (720 nm), and $TXH^{\cdot}$ radical (420 nm) were reported in the spectra of TX and DPA in acetonitrile [25]. More significantly, there still are different spectral assignments of $DPA^{\cdot+}$, *e.g.* at 670 nm in methanol [29], at ∼690 nm in radiolysis experiment [30] and in low-temperature matrix irradiation measurements [31, 32].

In this work, the dependence of self-quenching process of $^3TX^*$ and its reaction with DPA on the solvent has been investigated. A special attention has been paid to comparing the electron affinity of the $n\pi^*$ and $\pi\pi^*$ components. Steady-state and nanosecond time-resolved spectra and dynamics of TX were measured in several solvents, including the nonpolar solvent (CCl_4) and the polar solvents (CH_3CN, CH_3CN/CH_3OH, CH_3CN/H_2O). Additionally, the photochemistry of TX in strongly acid media was studied, since the $^3\pi\pi^*$ aromatic ketone could abstract hydrogen atom from environment [33−35]. Notably, with the sequence of CCl_4, acetonitrile, methanol and water, solvent polarity and hydrogen-donor ability are monotonically increasing [9, 33]. These solvents have been used to study the photophysical properties of aromatic carbonyl compounds in previous studies [9, 12, 33−36]. By comparing the dynamic behaviors of $^3TX^*$ in these solvents, the solvent dependence is discussed in detail. A minor aim of this work is to clarify the inconsistent spectral assignment of the absorption of $DPA^{\cdot+}$.

II. EXPERIMENTS

A. Equipment

Steady-state UV-visible absorption spectra were recorded on a Shimadzu UV-3600 spectrophotometer. Laser induced fluorescence measurements were carried out in a Hitachi F-4600 spectrophotometer. The nanosecond time-resolved experiments are performed on laser flash photolysis system [37]. Transient absorption spectra and triplet quenching data were collected using a Nd-YAG laser (PRO190, Spectra Physics) with 8 ns excitation pulses at 355 nm. The source of analytical light was a 500W Xenon lamp. The laser and analytical light beam perpendicularly passed through a flow quartz cuvette with an optical path length of 10 mm. After once passing the cell, the analytical light beam entered a monochromator equipped with a photomultiplier (CR131, Hamamatsu) at the rear of the exit slit. And the oscilloscope (TDS3052B, Tektronix) was used to record the signals from the photomultiplier.

B. Materials

TX and DPA were used without further purification, which were obtained from Alfa Aesar Co. The dominate solvents, CCl_4, CH_3CN, and CH_3OH, were high performance liquid chromatography grade quality. Water was purified through a Millipore Milli-Q system. Given the low solubility of TX in protic media, CH_3CN/CH_3OH and CH_3CN/H_2O solutions with different volume ratio were prepared by using the water. The pH of the solutions was adjusted with HCl solution. All samples were deaerated by high purity argon (99.99%) bubbling for 30 min. All the experimental data were collected at ∼25 °C. The concentration of TX is 0.5×10^{-3} mol/L

DOI:10.1063/1674-0068/cjcp2004048

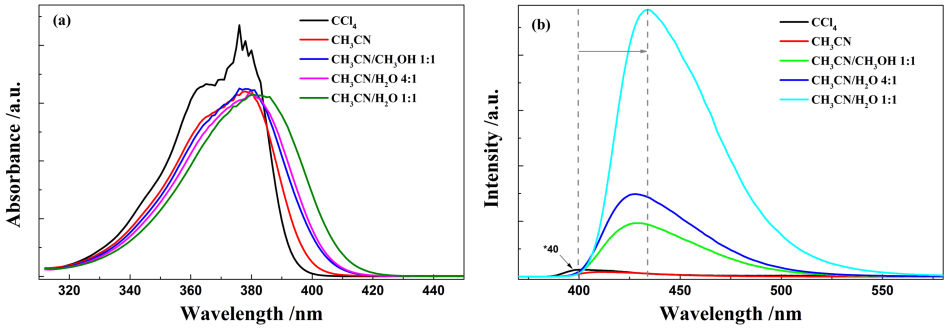

FIG. 1 (a) UV-visible and (b) fluorescence spectra of TX in different solvents, where the fluorescence intensity of TX in CCl_4 is magnified by a factor of 40 in order to be clearly compared with others.

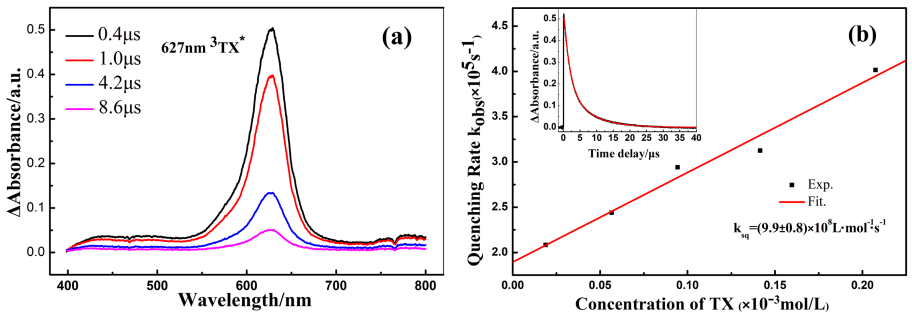

FIG. 2 (a) Transient absorption spectra of TX in CH_3CN, (b) the relationship between quenching rate of $^3TX^*$ and the concentration of TX in CH_3CN, the inserted panel shows the experimental and fitted decay curves (627 nm) of $^3TX^*$.

and that of DPA is 0.3×10^{-3} mol/L in all spectra.

III. RESULTS AND DISCUSSION

A. Steady-state spectra of TX

FIG. 1 shows the UV-visible and fluorescence spectra of TX. In FIG. 1(a), the intensities of the absorption bands are almost not changed, while a red-shift about 5 nm of the absorption maximum is observed with the sequence of CCl_4, acetonitrile, alcohol acetonitrile and aqueous acetonitrile. In addition, the major band profile of TX in CCl_4 is also similar except for the more distinct vibrational structure. In FIG. 1(b), with the solvent polarity and hydrogen-donor ability increasing, a red-shift about 34 nm of the fluorescence maximum is found, and the fluorescence intensities are significantly enhanced.

It is well known that the first absorption band of TX involves $n\pi^*$ and $\pi\pi^*$ states [8−10]. The energies of these two states could be influenced by the solvent polarity [12, 38]. However, in FIG. 1(a), the Franck-Condon excitation of $S_0\rightarrow S_1$ is almost not changed. Moreover, the important modes of deactivation of the $^1TX^*$ are fluorescence and ISC to the $^3TX^*$ [8, 9]. The great red-shift of fluorescence maximum implies that the $^1\pi\pi^*$ state is stabilized [10]. And with the solvent polarity and hydrogen-donor ability increasing, the significant improvement of fluorescence intensity is due to the decrease in ISC to $^3\pi\pi^*$ [8].

B. Time-resolved spectra of TX

FIG. 2(a) displays the transient absorption spectrum of TX in CH_3CN. In the spectrum, there is a wide absorption band at 627 nm, which is assigned to $^3TX^*$ [10, 25, 29]. As the delay time extending from 0.4 μs to 8.6 μs, the absorption intensities dramatically decrease. In addition, the small hollows at 467 and 766 nm in FIG. 2(a) are coming from the power flux of Xenon light.

By the least square fitting to the decay curve (627 nm), the quenching rate of $^3TX^*$ was obtained. The rates are monotonously increased as shown in FIG. 2(b). And in CH_3CN, the self-quenching rate constant k_{sq} is $(9.9\pm0.8)\times10^8$ $L\cdot mol^{-1}\cdot s^{-1}$ by linear fitting. The diffusion-controlling rate limit is 1.94×10^{10} $L\cdot mol^{-1}\cdot s^{-1}$, which is much larger than the k_{sq}. Therefore, an excimer is proposed to stabilize $^3TX^*$.

DOI:10.1063/1674-0068/cjcp2004048

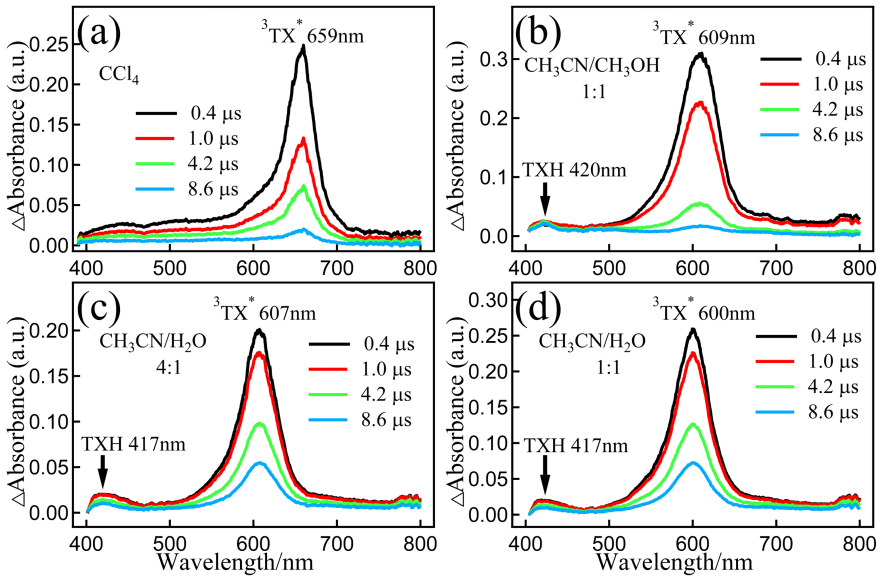

FIG. 3 Transient absorption spectra of TX in (a) CCl_4, (b) CH_3CN/CH_3OH (1:1), (c) CH_3CN/H_2O (4:1), and (d) CH_3CN/H_2O (1:1).

TABLE I The quenching rates k_{obs} ($\times 10^5$ s^{-1}) and corresponding absorption wavelength λ (in nm) of the intermediates after irradiation of TX in different solvents. Concentration of TX is 0.5×10^{-3} mol/L.

Solvent	TXH·		^{3}TX*	
	k_{obs}	λ	k_{obs}	λ
CCl_4	–	–	15.7±0.2	659±2
CH_3CN	–	–	5.0±0.1	627±2
CH_3CN:CH_3OH(1:1)	2.1±0.1	420±6	4.5±0.1	609±3
CH_3CN:H_2O(4:1)	2.1±0.1	417±6	3.4±0.1	607±3
CH_3CN:H_2O(1:1)	1.9±0.1	417±6	2.6±0.1	600±3

FIG. 3 shows the nanosecond time-resolved spectra of TX in CCl_4, CH_3CN/CH_3OH (1:1), CH_3CN/H_2O (4:1) and CH_3CN/H_2O (1:1) solvents. A blue-shift of the ^{3}TX* absorption maximum is observed from 659 nm in CCl_4, 609 nm in CH_3CN/CH_3OH (1:1), 607 nm in CH_3CN/H_2O (4:1) to 600 nm in CH_3CN/H_2O (1:1). As mentioned above, the $^1\pi\pi^*$ character becomes more dominant in the $S_0\rightarrow S_1$ transition in a polar solvent on irradiation. Thus ^{3}TX* exhibits enhanced $\pi\pi^*$ character especially in polar hydrogen bonding solvents. The recent calculation [8] indicates, the more polar solvents result in a bigger triplet-triplet transition energy of $^3\pi\pi^*$ state, which agrees well with the present blue-shift.

Table I displays the quenching rates of ^{3}TX*. Hydrogen bonds formed by the oxygen atom of the TX carbonyl group and hydroxylic groups of protic solvents already exist in the ground state [39]. Thus the direct hydrogen abstraction easily occurs in protic solvents. And in FIG.3 (b)−(d), there is a new absorption band at ∼420 nm, which is attributed to the TXH· radical according to the previous studies [10, 25, 29]. In Table I, the quenching rate of ^{3}TX* decrease gradually from CH_3CN/CH_3OH (1:1) to CH_3CN/H_2O (1:1). This can be attributed in part to the inherent lower reactivity of $^3\pi\pi^*$ state towards hydrogen abstraction [40, 41]. It is worth noting that the hydrogen-donor ability of H_2O is stronger than that of CH_3OH [9]. Therefore the stronger hydrogen bonding solvents result in a less reactive triplet and slower quenching rate.

Similarly, the k_{sq} in alcohol acetonitrile and that in aqueous acetonitrile are obtained through fitting the relationship of the ^{3}TX* quenching rate and the concentration of TX. In CH_3CN/CH_3OH (1:1) solvent, k_{sq} is $(8.0\pm0.7)\times10^8$ L·mol^{-1}·s^{-1}, and it is $(5.8\pm0.4)\times10^8$ L·mol^{-1}·s^{-1} in CH_3CN/H_2O (1:1) solvent. According to the hydrogen bonding effect between ^{3}TX* and hydroxylic group, an exciplex can be formed in a protic solvent which probably could influence the process of collisional quenching of ^{3}TX*. Thus the k_{sq} is reduced with the sequence of CH_3CN, CH_3CN/CH_3OH (1:1) and CH_3CN/H_2O (1:1).

Additionally, the quenching rate of triplet TX in CCl_4 is much faster than those in CH_3CN and protic solvents as shown in Table I. More significantly, the decay rate is monotonically increased with the concentration within

DOI:10.1063/1674-0068/cjcp2004048

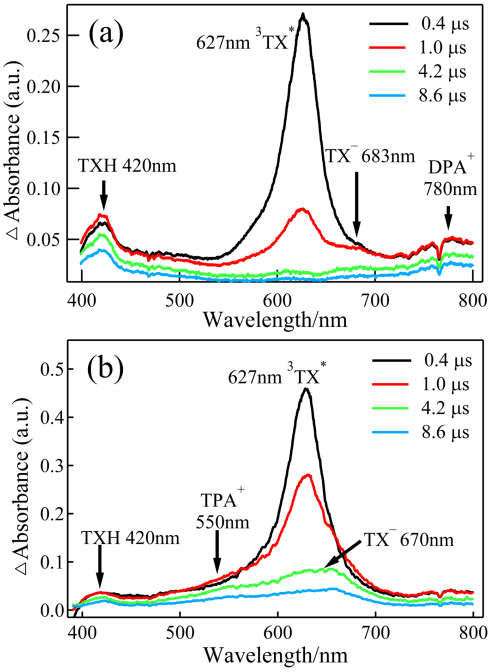

FIG. 4 Transient absorption spectra of TX in the presence of (a) DPA, (b) TPA in CH_3CN.

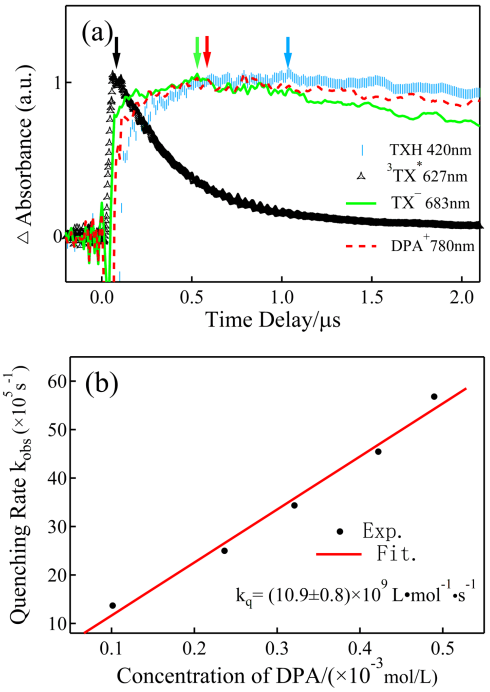

FIG. 5 (a) Decay curves of all intermediates after irradiation of TX in the presence of DPA in CH_3CN, and the arrows point to the absorption maximum, (b) the relationship between quenching rate of ^{3}TX* and the concentration of DPA in CH_3CN.

a range from 0.05×10^{-3} mol/L to 0.2×10^{-3} mol/L, and then decreases dramatically. Therefore, the excimer is proposed to be very important to stabilize the ^{3}TX*, especially in a high concentration.

C. Time-resolved spectra of TX in the presence of DPA in CH_3CN

FIG. 4(a) displays the nanosecond time-resolved spectra of TX in the presence of DPA in CH_3CN. The ^{3}TX* absorption (627 nm) intensity is significantly decreased compared to that in FIG. 2(a). And the absorption (420 nm) intensity of TXH$^\cdot$ radical is remarkably enhanced. Moreover, there are two new bands respectively at 683 nm and 780 nm, especially at 1.0 μs.

FIG. 5(a) shows the dynamic decays respectively at 420, 627, 683, and 780 nm. According to the delay time, ^{3}TX* is produced first after irradiation. Because of its quenching by DPA, the ^{3}TX* absorption intensity rapidly decreases, accompanied with the production of two intermediates (683 nm and 780 nm). And these two absorptions simultaneously reach the maximum at about 0.7 μs. Therefore the two intermediates are believed to be from the primary reaction between ^{3}TX* and DPA. Obviously, the absorption intensity of TXH$^\cdot$ radical reaches a maximum at last. Thus it must be from the secondary reaction between the two intermediates.

Table II summarizes the quenching rates of all the intermediates. As a common electron donor, DPA can provide an electron to ^{3}TX* [25, 27]. Therefore TX$^{\cdot-}$ and DPA$^{\cdot+}$ ions are believed to be from the primary electron transfer from DPA to ^{3}TX* as shown in Eq.(1). Then the absorption bands at 683 nm and 780 nm are attributed to TX$^{\cdot-}$ and DPA$^{\cdot+}$ ions. Considering the inconsistent spectral assignments of DPA$^{\cdot+}$ in previous studies, the nanosecond time-resolved spectra of TX in the presence of TPA in CH_3CN is measured as shown in FIG. 4(b). Because the absorption band of TPA$^+$ cation radical in CH_3CN is at 550 nm [42], the band at 780 nm is certainly attributed to DPA$^{\cdot+}$ cation in FIG. 4(a). It is worth noting that the wavelength range of DPA$^{\cdot+}$ cation absorption band is particularly wide. And it is difficult to identify its absorption maximum. This probably is the critical factor to cause the previous inconsistent spectral assignments.

TX$^{\cdot-}$ anion could capture a proton from DPA$^{\cdot+}$ cation as shown in Eq.(2). As the primary reaction product and the secondary reaction reactant, the quenching rate of TX$^{\cdot-}$ should be approximate to that of DPA$^{\cdot+}$. However, the slightly higher quenching rate

DOI:10.1063/1674-0068/cjcp2004048

TABLE II The quenching rates k_{obs} ($\times 10^5$ s^{-1}) and corresponding absorption wavelength λ of all intermediates after irradiation of TX and DPA mixture.

Solvent	Intermediate	λ/nm	k_{obs}
CH_3CN	$TXH^{\cdot}$	420±5	1.9±0.1
	$^3TX^*$	627±3	27.6±0.1
	$TX^{\cdot -}$	683±7	3.5±0.1
	$DPA^{\cdot +}$	780±8	2.4±0.1
CH_3CN/CH_3OH (9:1)	$TXH^{\cdot}$	420±6	2.1±0.1
	$^3TX^*$	618±5	30.3±0.1
	$TX^{\cdot -}$	676±8	4.1±0.1
	$DPA^{\cdot +}$	780±8	2.4±0.1
CH_3CN/CH_3OH (1:1)	$TXH^{\cdot}$	417±6	2.0±0.1
	$^3TX^*$	609±5	36.4±0.9
	$TX^{\cdot -}$	674±8	5.0±0.1
	$DPA^{\cdot +}$	780±8	2.4±0.1
CH_3CN/H_2O (1:1)	$TXH^{\cdot}$	418±6	1.5±0.1
	$^3TX^*$	600±5	29.1±0.1
	$TX^{\cdot -}$	673±9	2.9±0.1
	$DPA^{\cdot +}$	780±8	1.7±0.1

Note: concentration of TX is 0.5×10^{-3} mol/L and concentration of DPA is 0.3×10^{-3} mol/L.

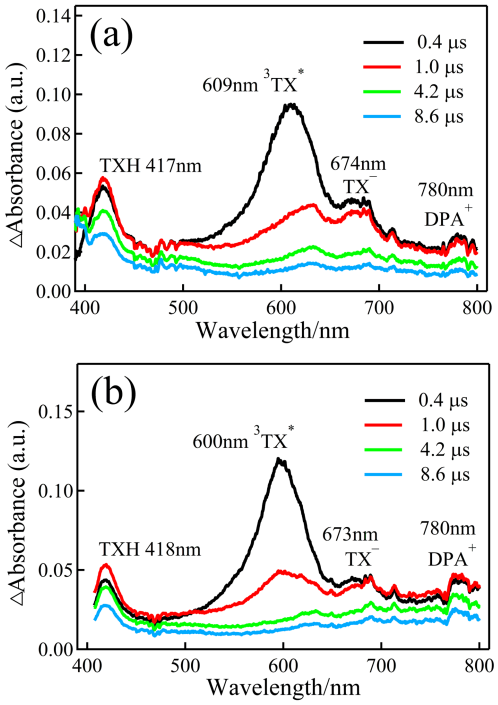

FIG. 6 Transient absorption spectra of TX and DPA in (a) CH_3CN/CH_3OH (1:1) (b) CH_3CN/H_2O (1:1).

of $TX^{\cdot -}$ may be ascribed to the influence of the nearby $^3TX^*$.

$$^3TX^* + DPA \rightarrow TX^{\cdot -} + DPA^{\cdot +} \quad (1)$$

$$TX^{\cdot -} + DPA^{\cdot +} \rightarrow TXH^{\cdot} + DPA_{-H} \quad (2)$$

Eq.(3) displays the Stern-Volmer relationship. By fitting with the relationship, the quenching rate constant k_q of $^3TX^*$ is determined as $(1.09\pm0.08)\times10^{10}$ $L\cdot mol^{-1}\cdot s^{-1}$, which is approximate to the encounter-controlled rate limit in CH_3CN. Obviously, the electron transfer from DPA to $^3TX^*$ is very effective indeed.

$$k_{obs} = k_0 + k_q[DPA] \quad (3)$$

where k_{obs} and k_0 are the quenching rate of $^3TX^*$ in the presence and absence of DPA, respectively.

D. Time-resolved spectra of TX and DPA in hydrogen bonding solvents

FIG. 6 shows the nanosecond time-resolved spectra of TX in the presence of DPA in CH_3CN/CH_3OH (1:1) and CH_3CN/H_2O (1:1). The absorption maximum at 609 nm or 600 nm is still assigned to $^3TX^*$. The absorptions at ~418 nm, ~673 nm and 780 nm are attributed to $TXH^{\cdot}$, $TX^{\cdot -}$ and $DPA^{\cdot +}$ respectively.

Similar to the quenching in CH_3CN, the two-step electron-proton transfer between $^3TX^*$ and DPA is also expected in protic solvents. Table II shows the quenching rates of all the intermediates. For the electron transfer from DPA to $^3TX^*$, the quenching rate constant k_q is very important to present the solvent dependence on its decay dynamics. In FIG. 7 the observed quenching rates of $^3TX^*$ monotonically increase with the DPA concentration in CH_3CN/CH_3OH (1:1) or CH_3CN/H_2O (1:1), and a linear relationship is obvious. The k_q can be determined as $(10.2\pm0.6)\times10^9$ $L\cdot mol^{-1}\cdot s^{-1}$ (in CH_3CN/CH_3OH) and $(9.6\pm0.7)\times10^9$ $L\cdot mol^{-1}\cdot s^{-1}$ (in CH_3CN/H_2O), both of which are proximately equal to the encounter-controlled rate limit. Thus the predominant deactivation of $^3TX^*$ is still via the quenching by DPA indeed. Moreover, the lowest excited $^3n\pi^*$ and $^3\pi\pi^*$ states of TX exist with different population ratio in different solvents. However, the quenching rates of $^3TX^*$ are almost the same in all mediums, although the direct hydrogen abstraction from methanol (or H_2O) by $^3TX^*$ is involved. Thus water or methanol probably plays an insignificant role in the electron transfer from DPA to $^3TX^*$. And the ability to capture electron of

DOI:10.1063/1674-0068/cjcp2004048

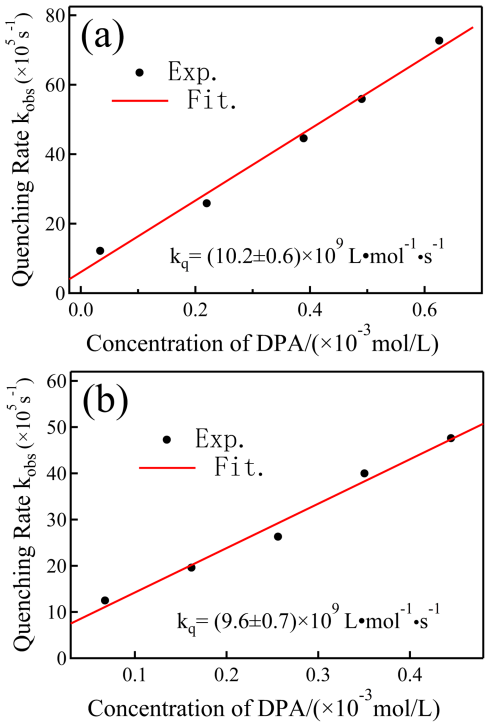

FIG. 7 The relationship between quenching rate of ^{3}TX* and the concentration of DPA in (a) CH_3CN/CH_3OH (1:1) and (b) CH_3CN/H_2O (1:1).

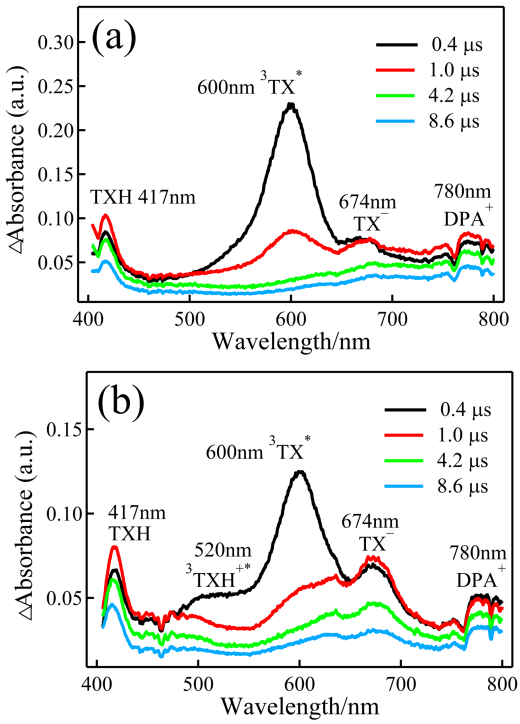

FIG. 8 Transient absorption spectra of TX and DPA in acidic CH_3CN/H_2O (1:1) solvent, (a) pH=5.0 and (b) pH=3.0.

the $^3n\pi^*$ excited state of TX is approximately equal to that of $^3\pi\pi^*$ state.

Additionally, as the products of the title reaction between ^{3}TX* and DPA, the quenching rates of $TX^{\cdot-}$ anion radical and $DPA^{\cdot+}$ cation radical should be close as both of them are produced and quenched simultaneously. Whereas the quenching rate of $TX^{\cdot-}$ is slightly accelerated with the molecular ratio of methanol increasing as shown in Table II, while that of $DPA^{\cdot+}$is kept constantly. Since a hydrogen bond can be formed between hydroxyl moiety of methanol and $TX^{\cdot-}$ anion, the proton transfer probably occurs as Eq.(4). Therefore the more methanol exists, the faster the decay rate of $TX^{\cdot-}$ is. However in the aqueous acetonitrile (1:1), the rate of $TX^{\cdot-}$ shows an opposite and abnormal behavior. It is even slower than that in CH_3CN, although the proton-transfer also probably occurs between $TX^{\cdot-}$ and water. A probable reason is due to the higher bond energy of hydroxyl in water than that in methanol, and thus the proton transfer from H_2O to $TX^{\cdot-}$ is restrained to a neglectable rate. Therefore, an interesting solvent dependence is found in the dynamic decay of $TX^{\cdot-}$ anion radical, although the dominant electron/proton transfer between ^{3}TX* and DPA is insusceptible.

$$TX^{\cdot-}+CH_3OH \rightarrow TXH^{\cdot}+CH_3O^- \qquad (4)$$

E. Time-resolved spectra of TX and DPA in acid aqueous acetonitrile solvents

In pH=5.0 CH_3CN/H_2O (1:1) solvent, the transient absorption spectra of TX and DPA are shown in FIG. 8(a). The major spectral features are very similar to those in CH_3CN/H_2O (1:1). In addition, the quenching rates of the intermediates in Table III are also approximately equal to those in CH_3CN/H_2O (1:1). Therefore the reaction mechanism of ^{3}TX* and DPA in pH=5.0 solvent is still kept as a two-step process as described by Eq.(1) and Eq.(2), and the hydrated proton does not markedly affect the electron and proton transfer between ^{3}TX* and DPA.

However, the transient absorption spectra are notably changed when pH value of TX and DPA mixture solution is changed from 5.0 to 3.0 as shown in FIG. 8(b). Besides four bands in FIG. 8(a), a new absorption band at 520 nm can be observed indicating that there is a new intermediate formed.

DOI:10.1063/1674-0068/cjcp2004048

TABLE III The quenching rates k_{obs} ($\times 10^5$ s^{-1}) and corresponding absorption wavelength λ of all intermediates after irradiation of TX and DPA mixture. Concentration of TX is 0.5×10^{-3} mol/L and that of DPA is 0.3×10^{-3} mol/L.

pH	Intermediates	λ/nm	k_{obs}
pH=5.0	$TXH^{\cdot}$	417±4	1.2±0.1
	$^3TXH^{+*}$	–	–
	$^3TX^*$	600±5	26.6±0.1
	$TX^{\cdot-}$	674±9	2.1±0.1
	$DPA^{\cdot+}$	780±8	1.2±0.1
pH=3.0	$TXH^{\cdot}$	417±3	1.2±0.1
	$^3TXH^{+*}$	520±9	13.4±0.5
	$^3TX^*$	600±5	45.7±0.1
	$TX^{\cdot-}$	674±7	2.1±0.1
	$DPA^{\cdot+}$	780±8	0.4±0.1

It is well known that the ground state of aromatic carbonyl compound is protonated in strongly acid media [34]. Thus there is a dynamic equilibrium between protonated and unprotonated TX in acidic solvent, and TXH^+ coexists with TX in solution. Once photolysis, $^3TX^*$ and $^3TXH^{+*}$ are produced immediately via Franck-Condon excitation of $S_0\rightarrow S_1$ and intersystem crossing of $S_1\rightarrow T_1$. Based on the spectral assignments in FIG. 8(a), the new absorption at 520 nm can be confessedly attributed to $^3TXH^{+*}$. Therefore an additional reaction between $^3TXH^{+*}$ and DPA is able to occur that $^3TXH^{+*}$ can also directly capture an electron from DPA to produce $TXH^{\cdot}$ radical as Eq.(5).

$$^3TXH^{+*} + DPA \rightarrow TXH^{\cdot} + DPA^{\cdot+} \quad (5)$$

$$^3TX^* + H_3O^+ \rightarrow {}^3TXH^{+*} + H_2O \quad (6)$$

By fitting the decay curve of $^3TX^*$ in pH=3.0, the quenching rate is determined as $(45.7\pm0.1)\times10^5$ s^{-1}, which is much higher than that in pH=5.0 or neutral solvent. The protonation of $^3TX^*$ as Eq.(6) should accelerate the quenching of $^3TX^*$. In Table III the quenching rate of $^3TXH^{+*}$ by DPA is $(13.4\pm0.5)\times10^5$ s^{-1} which is lower than that of $^3TX^*$ by DPA in pH=5.0 or neutral solvent. It indicates that the reduction potential of $^3TXH^{+*}$ is lower than that of $^3TX^*$, although there are no experimental values in references.

IV. CONCLUSION

The solvent dependence of the photophysical and photochemical behaviors of TX has been performed using nanosecond transient absorption spectroscopy. In the spectra of TX in CH_3CN, there is an unique absorption band at 627 nm, which is attributed to $^3TX^*$. In the hydrogen bonding solvent, there is a new weak absorption band at ∼420 nm in the spectra of TX, and it is assigned to $TXH^{\cdot}$ radical, which is produced via a direct hydrogen abstraction of $^3TX^*$ from the solvent. The self-quenching rate constant k_{sq} of $^3TX^*$ is reduced with the sequence of CH_3CN, CH_3CN/CH_3OH(1:1) and CH_3CN/H_2O(1:1). This may be due to the fact that the exciplex being formed by hydrogen bonding effect probably could influence the process of collisional quenching of $^3TX^*$.

The reaction mechanism between $^3TX^*$ and DPA happens via a two-step process of the electron/proton transfer. The bands at ∼683 nm and ∼780 nm in CH_3CN are assigned to $TX^{\cdot-}$ anion radical and $DPA^{\cdot+}$ cation radical, respectively. The quenching rate constant k_q is $(10.9\pm0.8)\times10^9$ $L\cdot mol^{-1}\cdot s^{-1}$ (in CH_3CN), $(10.2\pm0.6)\times10^9$ $L\cdot mol^{-1}\cdot s^{-1}$ (in CH_3CN/CH_3OH) and $(9.6\pm0.7)\times10^9$ $L\cdot mol^{-1}\cdot s^{-1}$ (in CH_3CN/H_2O), respectively. Obviously, the above rate constants are close indeed. Moreover, the quenching rates of $^3TX^*$ are almost the same in all mediums. Obviously, the solvent effect on the electron transfer from DPA to $^3TX^*$ is not significant, which suggests the ability to capture electron of the $^3n\pi^*$ excited state of TX is approximately equal to that of $^3\pi\pi^*$ state.

In addition, a solvent dependence is found in the dynamic decay of a primary product of $TX^{\cdot-}$ anion radical. Since a hydrogen bond can be formed between hydroxyl moiety and $TX^{\cdot-}$, the proton transfer probably occurs. And the bond energy of hydroxyl in water is higher than that of methanol. Thus the quenching rate of $TX^{\cdot-}$ anion is slightly accelerated with the molecular ratio of methanol in the mixture solvent increasing, while the rate is reduced in the aqueous acetonitrile.

When pH value of TX and DPA mixture solution is 5.0, the reaction mechanism of $^3TX^*$ and DPA is still a two-step process, and the hydrated proton does not markedly affect the electron and proton transfer. When pH value is 3.0, a dynamic equilibrium between protonated and unprotonated TX is definitely observed. Once photolysis, $^3TX^*$ and $^3TXH^{+*}$ are produced simultaneously. And a new band at 520 nm is obvious, which is attributed to the absorption of $^3TXH^{+*}$. Interestingly, the quenching rate of $^3TXH^{+*}$ by DPA is lower than that of $^3TX^*$ by DPA in pH=5.0 or neutral

DOI:10.1063/1674-0068/cjcp2004048

solvent, which indicates that the reduction potential of $^3TXH^{+*}$ is lower than that of $^3TX^*$.

V. ACKNOWLEDGMENTS

This work was supported by the Educational Commission of Anhui Province of China (No.KJ2018A0491). Lin Wang is also grateful for the financial support of Anhui Natural Science Foundation (No.1908085MB50).

[1] J. C. Dalton and F. C. Mongomery, J. Am. Chem. Soc. **96**, 6230 (1974).
[2] J. C. Scaiano, J. Am. Chem. Soc. **102**, 7747 (1980).
[3] C. Ley, F. Morlet-Savary, P. Jacques, and J. P. Fouassier, Chem. Phys. **255**, 335 (2000).
[4] M. V. Encinas, A. M. Rufs, T. Corrales, F. Catalina, C. Peinado, K. Schmith, M. G. Neumann, and N. S. Allen, Polymer **43**, 3909 (2002).
[5] X. T. Zhao, W. Q. Huang, D. D. Song, R. X. Lin, H. Huang, J. J. Huang, B. Wu, Y. G. Huang, and G. D. Ye, J. Mol. Model. **26**, 56 (2020).
[6] S. Kayal, K. Roy, Y. A. Lakshmanna, and S. Umapathy, J. Phys. Chem. A **122**, 6048 (2018).
[7] R. Mundt, T. Villnow, C. T. Ziegenbein, P. Gilch, C. Marianb, and V. R. Constapel, Phys. Chem. Chem. Phys. **18**, 6637 (2016).
[8] G. Angulo, J. Grilj, E. Vauthey, l. Serrano-Andres, O. Rubio-Pons, and P. Jacques, Chem. Phys. Chem. **11**, 480 (2010).
[9] E. Krystkowiak, A. Maciejewski, and J. Kubicki, Chem. Phys. Chem. **7**, 597 (2006).
[10] G. C. Ferreira, C. C. Schmitt, and M. G. Neumann, J. Braz. Chem. Soc. **17**, 905 (2006).
[11] R. W. Yip, A. G. Szabo, and P. K. Tolg, J. Am. Chem. Soc. **95**, 4471 (1973).
[12] M. G. Neumann, M. H. Gehlen, M. V. Encinas, N. S. Allen, T. Corrales, C. Peinado, and F. Catalina, J. Chem. Soc. Fraday Trans. **93**, 1517 (1997).
[13] S. F. Yates and G. B. Schuster, J. Org. Chem. **49**, 3349 (1984).
[14] J. P. Fouassier and S. K. Wu, J. Appl. Polym. Sci. **44**, 1779 (1992).
[15] J. P. Fouassier and D. Ruhlmann, Eur. Polym. J. **29**, 505 (1993).
[16] J. P. Fouassier, D. J. Lougnot, I. Zuchowicz, P. N. Green, H. J. Timpe, K. P. Kronfeld, and V. J. Muller, Photochem. **36**, 347 (1987).
[17] N. S. Allen, E. M. Howells, E. Lam, F. Cataline, P. N. Green, W. A. Green, and W. Chen, Eur. Polym. J. **24**, 591 (1988).
[18] D. J. Lougnot, C. Turck, and J. P. Fouassier, Macromolecules **22**, 108 (1989).
[19] N. S. Allen, F. Cataline, J. L. Mateo, R. Sastre, W. Chen, P. N. Green, and W. A. Green, Polym. Mater. Sci. Eng. **60**, 10 (1989).
[20] N. Mataga, M. Ottolenghi, *Molecular Association*, Vol. 2, R. Forster, Ed., New York: Academic Press, 1 (1979).
[21] A. Z. Weller, Phys. Chem. (Munich), **130**, 129 (1982).
[22] T. Okada, T. Mori, and N. Mataga, Bull. Chem. Soc. Jpn. **49**, 3398 (1976).
[23] S. F. Yates and G. B. Schuster, J. Org. Chem. **49**, 3349 (1984).
[24] J. P. Fouassier and D. J. Lougnot, J. Appl. Polym. Sci. **34**, 477 (1987).
[25] F. Scigalski and J. Paczkowski, Macromol. Chem. Phys. **209**, 1872 (2008).
[26] S. G. Cohen, A. Parola, and G. H. Parsons, Chem. Rev. **73**, 141 (1973).
[27] Q. Q. Zhu, W. Schnabel, and P. Jacques, J. Chem. Soc., Faraday Trans. **87**, 1531 (1991).
[28] X. S. Jiang and J. Yin, Polymer **45**, 5057 (2004).
[29] Q. Sun, J. T. Wang, L. M. Zhang, and M. P. Yang, Acta Phys. Chim. Sin. **26**, 2481 (2010).
[30] G. N. Lewis and D. Lipkin, J. Am. Chem. Soc. **64**, 2801 (1942).
[31] R. Rahn, J. Schroeder, J. Troe, and K. H. Grellmann, J. Phys. Chem. **93**, 7841 (1989).
[32] T. Shida, Y. Nosaka, and T. Kato, J. Phys. Chem. **82**, 695 (1978).
[33] C. H. Evans, N. Prud'homme, M. King, and J. C. Scaiano, J. Photochem. Photobiol. A **121**, 105 (1999).
[34] R. Rusakowicz, G. W. Byers, and P. A. Leermakers, J. Am. Chem. Soc. **93**, 3263 (1971).
[35] N. S. Allen (Ed.), *Photopolymerization and Photoimaging Science and Technology*, Applied Science, London, New York: Elsevier, (1989).
[36] J. C. Scaiano, J. Am. Chem. Soc. **102**, 7747 (1980).
[37] L. Chen, Q. H. Zhou, X. Liu, X. G. Zhou, and S. L. Liu, Chin. J. Chem. Phys. **28**, 4 (2015).
[38] J. J. Cavaleri, K. Prater, and R. M. Bowman, Chem. Phys. Lett. **259**, 495 (1996).
[39] H. Morita, S. Mori, and T. Yamaoka, Bull. Chem. Soc. Jpn. **61**, 191 (1988).
[40] M. V. Encina, E. A. Lissi, E. Lemp, A. Zanocco, and J. C. Scaiano, J. Am. Chem. Soc. **105**, 1856 (1983).
[41] A. Gilbert and J. Baggot, *Essentials of Molecular Photochemistry*, London: Blackwell Scientific Publications, (1991).
[42] R. F. Bartholomew, R. S. Davidson, P. F. Lambeth, J. F. McKellar, and P. H. Turner, J. Chem. Soc. Perkin Trans. **2**, 577 (1972).

DOI:10.1063/1674-0068/cjcp2004048